Filterless Reception of Terabit, Faster Than Nyquist Superchannels With 4 GHz Electronics

Abhinand Venugopalan , *Graduate Student Member, IEEE*, Paulomi Mandal , Janosch Meier ,
Karanveer Singh , and Thomas Schneider

Abstract—Data transmission speeds in excess of 1 Terabit per second (Tbit/s) are predicted with the evolving needs of modern applications, ranging from new communication technologies to data intensive computing and emerging paradigms like internet-of-things and augmented reality. The bandwidth limitation of current electronics, however, may represent a critical challenge in achieving such high data rates. Here, we experimentally demonstrate how, with the help of photonics, a single faster than Nyquist (FTN) superchannel with a 3-dB bandwidth of 662.5 GHz and a data rate in excess of 1 Tbit/s can be detected and processed with just 4 GHz electronics. The method does not need any kind of filter, optical delay line, pulse source, electronic post processing or other sophisticated electronic or photonic equipment. It is simply based on orthogonal sampling in a Mach-Zehnder modulator (MZM) by sinc-pulse sequences. Therefore, it has the potential to be integrated into any photonic platform. The presented approach may be a straight-forward solution to meet the demands of future terabit communication and measurement systems with cost-effective, integrated devices.

Index Terms—Data communication, high-speed transmission, optical modulation, orthogonal sampling, faster than Nyquist signaling.

I. INTRODUCTION

THE unpredictable demand for global internet connectivity, especially during the Covid-19 pandemic, has led to an increase in the required bandwidths for data centers and worldwide communication systems to support remote access for work and education, video conferencing, online gaming, factory automation, autonomous driving, the Internet of Things and streaming, to name just a few [1], [2]. For data centers, data rates of 400 Gbit/s are already being deployed, and it is predicted that they will go beyond 1 Tbit/s in the near future [3], [4]. Even for the wireless access to the communication systems via 6 G and beyond, peak data rates of 1 Tbit/s are envisioned [5]. To meet

the growing demand for high-speed data traffic, current solutions increase the spectral efficiency of the modulation format, they use advanced scaling or multiplexing together with sophisticated error correction, or they simply incorporate new communication hardware like few mode and few core fibers [6]. However, all of these solutions are accompanied by a complex, power hungry signal processing [7].

To detect and process a 1 Tbit/s signal, limited to its Nyquist bandwidth, with 28% overhead for the forward error correction [3] transmitted using dual-polarization and 16-quadrature amplitude modulation (16-QAM), for instance, requires a receiver with a bandwidth of 80 GHz, which is far beyond the abilities of the standard complementary metal-oxide semiconductor (CMOS) technology. Other materials like InP and SiGe offer higher bandwidths [8], [9], [10]. However, this leads to challenges in terms of seamless integration with the following CMOS based digital signal processing (DSP) [11]. Another severe problem for the reception of high-bandwidth signals is the aperture jitter in the electronic sample and hold circuit based analog-to-digital converters (ADCs) [12]. The sample and hold circuit can be seen as a switch, which samples the current amplitude value and keeps it constant for a while. But after the clock signal has been received by the circuit, it is uncertain when the sample and hold really opens or closes. Although extremely precise clocks with jitter values in the zeptosecond (10^{-21} s) range have been shown [13], state of the art ADCs show jitter values of only 100 fs (10^{-13} s) [14]. The jitter reduces the effective number of bits (ENOB) of the ADC for higher bandwidths and therefore, the tolerance of the receiver against the signal-to-noise ratio, especially for spectrally efficient, high-symbol rate signals.

High-bandwidth signal detection up to several hundreds of GHz has been reported in [15], [16], [17]. In [15] and [16], signals with bandwidths exceeding 100 GHz were detected through a spectrally sliced coherent detection. This technique utilizes optical filters to decompose a broadband signal into several spectral slices, individually detected using an optical frequency comb as a multi-wavelength local oscillator (LO). In [16], for instance, a coherent receiver with a bandwidth of 228 GHz is implemented using optical filters and an array of photodetectors, processing slices of individual optical bandwidths of 40 GHz to detect a 214 GBd dual-polarization quadrature phase shift keying (QPSK) signal with a line rate of 856 Gbit/s. Such methods heavily depend on high-quality optical filters for the spectral slicing of the optical signal. These
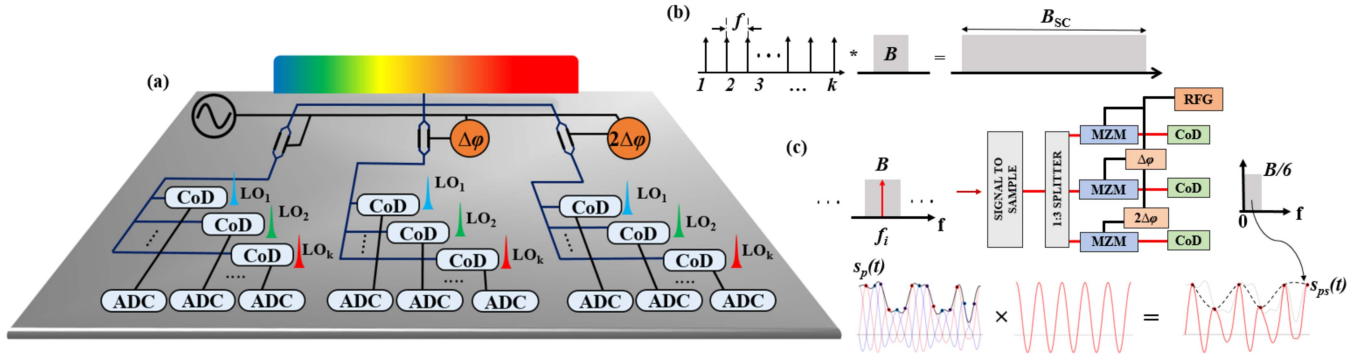
Fig. 1.   Schematic illustration of the proposed system (a). The incoming high-bandwidth signal with the bandwidth B_{SC} is split into three branches, each equipped with an MZM. By driving the MZMs with a phase-shifted, sinusoidal radio frequency, the incoming high-bandwidth signal is sampled orthogonally. This down-converts each spectral slice with an optical bandwidth B into three sub-signals, which can then be detected and processed with coherent detectors (CoDs) and electronics with a baseband bandwidth of $B/6$ (c). To process all spectral slices simultaneously, each CoD is driven with a comb line from a frequency comb as LO. Since the frequency spacing between the comb lines is six times higher than the bandwidth of the CoD, no filter is needed to separate the slices. The comb consists of k lines (b) and defines the overall bandwidth of the incoming signal with $B_{SC} = kB$ and the number of spectral slices k.

filters introduce additional insertion loss and make the overall schemes challenging to miniaturize. An alternative approach without optical slicing filters is presented in [17], showcasing a waveform measurement in a bandwidth exceeding 600 GHz with optical frequency combs as multi-wavelength LOs. This method involves an array of inphase/quadrature receivers fed by the complete optical waveform and by time-delayed copies of the full LO comb. However, the signal spectrum includes bandgaps within the individual slices, compromising spectral efficiency within the available 600 GHz band. Moreover, variable optical delay lines and balanced photodiodes with bandwidths up to 100 GHz were also employed, making the integration very challenging.

Here, we experimentally demonstrate the detection of a signal with a bandwidth of 662.5 GHz and achieve a data rate of up to 1.485 Tbit/s. To the best of our knowledge, this is the highest bandwidth that has been detected and processed in an experiment [17]. Additionally, the coherent receiver consists of photodiodes and electronics with a bandwidth of only 4 GHz and is based on parallel orthogonal sampling in a MZM [18], [19]. The parallel sampling divides the high-bandwidth optical signal into several low-bandwidth ones, which can then be processed using low-speed electronics. Due to this bandwidth reduction, the signal can be processed with a higher signal-to-noise and distortion ratio (SINAD) and corresponding ENOB value [20], which enables higher spectral efficiencies and may reduce the power consumption for subsequent electronic signal processing. Moreover, we do not have any guard bands inside the 662.5 GHz bandwidth and show a symbol rate of 742.5 GBd, corresponding to a 12% FTN transmission. Therefore, the presented concept might be able to solve the bandwidth bottleneck problem of receivers for future communication systems.

The article is structured as follows. In Section II, the concept is explained. Section III describes the experimental setup and presents the results. Finally, a brief discussion about the proposed system in Section IV followed by a conclusion in Section V is given.

II. CONCEPT

A schematic representation of the high-bandwidth receiver is shown in Fig. 1(a). Although the broadband signal has no guard-bands in the spectrum, we assume that the overall optical bandwidth B_{SC} consists of k spectral slices with the bandwidth B so that; $B_{SC} = kB$ (please see Fig. 1(b)). First, the power of the signal with the whole optical bandwidth B_{SC} is split into three branches and orthogonally sampled by sinc-pulse sequences in an MZM [18], [19]. This sampling is described for a single slice in more detail in Fig. 1(c). In accordance with the sampling theorem, each bandwidth-limited signal can be seen as a summation of time-shifted sinc pulses, weighted with the sampling values. Therefore, each sampling value can be retrieved by an integration of the multiplication of the signal with a sinc pulse with the right bandwidth and time shift. Unfortunately, sinc pulses are just a mathematical construct and cannot be generated in a practical system. Alternatively, each signal can as well be described as a superposition of time-shifted, orthogonal sinc-pulse sequences periodically weighted with the sampling values [12] as shown with $s(t)$ in Fig. 1(c). A sinc-pulse sequence with the repetition rate $\frac{1}{\Delta f}$ and duration $\frac{1}{N\Delta f}$, from the peak to the first zero crossing, corresponds to a flat, phase-locked frequency comb of N lines and spacing Δf, with a comb bandwidth of $B = N\Delta f$ in the frequency domain [21]. Mathematically, such a sinc-pulse sequence can be described by the following equation:

$$\mathrm{sq}_{N,B}(t) := \lim_{\substack{x \to t \\ \frac{Bx}{N} \in \mathbb{R} \backslash \mathbb{Z}}} \left(\frac{\sin(\pi B x)}{N \sin\left(\frac{\pi B x}{N}\right)} \right)$$

$$= \frac{2}{N} \left(\frac{1}{2} + \sum_{l=1}^{\frac{N-1}{2}} \cos\left(\frac{2\pi l B t}{N} \right) \right)$$

$$= \sum_{l=-\infty}^{\infty} \mathrm{sinc}(Bt - lN). \qquad (1)$$

Therefore, a sinc-pulse sequence (second term in (1)) is the superposition of N cosine functions with a spacing of Δf (third

term) and equivalently it is the superposition of an unlimited number of ideal sinc pulses (fourth term):

$$\text{sinc}(t) := \lim_{\substack{x \to t \\ x \in \mathbb{R} \backslash \{0\}}} \left(\frac{\sin(\pi x)}{\pi x} \right). \qquad (2)$$

In the frequency domain, the sinc function corresponds to a rectangular function:

$$[\mathcal{F}_t(\text{sinc}(t))] (f) = \Pi(f). \qquad (3)$$

Thereby, $\mathcal{F}_t$ is the Fourier transform and $\Pi(f) = 1$ for $|f| < 1/2$, $1/2$ for $|f| = 1/2$ and 0 elsewhere [19]. All the superimposed ideal sinc pulses in the last term of (1) have the same bandwidth, B, and are time shifted to each other, so that the maximum of the following pulse is in the N-th zero crossing of the previous one. This superposition of the unlimited pulses is possible without any kind of inter-symbol-interference between them, because they are orthogonal to each other [21].

Here we have restricted the number of comb lines to $N = 3$. Such a flat three-line frequency comb can be achieved by using an intensity modulator and adjusting the bias and radio frequency (RF) voltage driving the modulator in a way that the carrier and sidebands have the same amplitude [21], [22]. As depicted in Fig. 1(c), by multiplying the spectral slices with a sinc-pulse sequence of the right time shift, periodical sampling values with $1/3^{\text{rd}}$ of the original sampling rate and $1/6^{\text{th}}$ of the baseband bandwidth can be retrieved. The sinc-pulse sequence generation and multiplication is carried out simultaneously in one single MZM. To get the whole information of the slice, two more orthogonal sinc-pulse sequences have to be multiplied. For orthogonality, these sinc-pulse sequences have to be time shifted to the zero crossings of the first one. For the sampling with the 3-line sinc-pulse sequences, since just a single RF tone is required, the orthogonality between parallel branches can be realized through a phase shift of the driving frequency of the modulator, which can be adjusted very precisely in the electrical domain. However, experiments and simulations have shown that a slight phase change of the sine wave driving the modulators still leads to very good results [18].

In the experiments we create a superchannel $s_{\text{SC}}(t)$ with a bandwidth B_{SC} by a superposition of k-spectral slices. The whole transmission signal is described by all the spectral slices together with the respective carriers, of angular frequency ω_p and phase φ_p, as follows:

$$s_{\text{SC}}(t) = \sum_{p=1}^{k} s_p(t) \cdot \cos \left(\omega_p \cdot t + \varphi_p \right). \qquad (4)$$

The p-th slice $s_p(t)$, with a baseband bandwidth of $B/2$, can be written in accordance to the sampling theorem as follows [23]:

$$s_p(t) = \sum_{m=-\infty}^{\infty} s \left(\frac{m}{B} \right) \cdot \text{sinc}(Bt - m). \qquad (5)$$

According to (5), each single slice can be described as a superposition of time-shifted, sinc pulses of bandwidth B, each of which weighted with a single sampling value. The same signal can be described as the superposition of time-shifted, sinc-pulse sequences, each of which periodically weighted with $1/N$-th of the sampling values:

$$s_p(t)$$
$$= \sum_{m=-\infty}^{\infty} \sum_{l=1}^{N} \left[\mathcal{F}_f^{-1} \left(\left[\mathcal{F}_t \left(s_p(t) \cdot \text{sq}_{N,B} \left(t - \frac{l-1}{B} \right) \right) \right] (f) \right. \right.$$
$$\left. \left. \cdot \Pi \left(\frac{Nf}{B} \right) \right) \right] \left(\frac{l-1}{B} + \frac{mN}{B} \right) \cdot N$$
$$\cdot \text{sinc}(Bt - (l-1) - mN). \qquad (6)$$

As single sinc pulses, sinc-pulse sequences are orthogonal to each other. Therefore, $1/(kN)$-th of the whole information of the superchannel can be retrieved by a multiplication of the superchannel with a sinc-pulse sequence with the right bandwidth and time shift, followed by a coherent detection with a local oscillator signal with one of the ω_p center frequencies in a low-bandwidth $B_{\text{SC}}/(2kN) = B/(2N)$ coherent detector. If the whole information of the superchannel has to be detected in real time, $k \cdot N$ parallel branches are necessary. But, each of these branches only needs low bandwidth electronics reduced to $B_{\text{SC}}/(2kN)$.

In Fig. 1(a), all spectral slices of the incoming signal are orthogonally sampled in the three branches simultaneously. Therefore, the optical bandwidth and sampling rate of all the slices has been reduced by 3 for each of the three branches. Since the baseband width is half the optical bandwidth, the information in the single branch can be retrieved with a CoD and a following electronic signal processing with a bandwidth of $B/6$.

Each of the parallel CoDs is driven with a single line from a frequency comb as LO. For each CoD, the frequency of this line should be in the vicinity of one of the slice centers. The spacing between the comb lines is f and corresponds to the optical bandwidth of the slice B. Therefore, it is six times higher than the bandwidth of the down-converted sub-signal. Due to the huge bandwidth difference, no optical or electronic filter is needed. The other two sub-signals from this and all the other slices can be detected in the branches with a phase shift of $120°$ and $240°$ by parallel coherent detection with the comb lines. Of course, the bandwidth difference can further be increased and the required bandwidth of the photodiode and the CoD can further be reduced by increasing the value of N [18].

III. EXPERIMENT AND RESULTS

A. Experiments

A schematic illustration of the experimental setup is shown in Fig. 2. Since we cannot generate signals with very high bandwidth in our lab, we were using equidistant, flat spectral lines from an optical frequency comb as carriers for data modulation. The output of a fiber laser centered at 193.40 THz is converted to a frequency comb by a Fabry-Perot electro-optic phase modulator, which acts as an OCG. The input RF and bias to the OCG determines the spacing and number of lines in the frequency comb. Since the comb spectrum of the OCG is triangular, individual comb lines are selectively attenuated to generate a flat comb by using a waveshaper (Finisar-1000 s) as programmable filter. In the first set of experiments, 25 lines
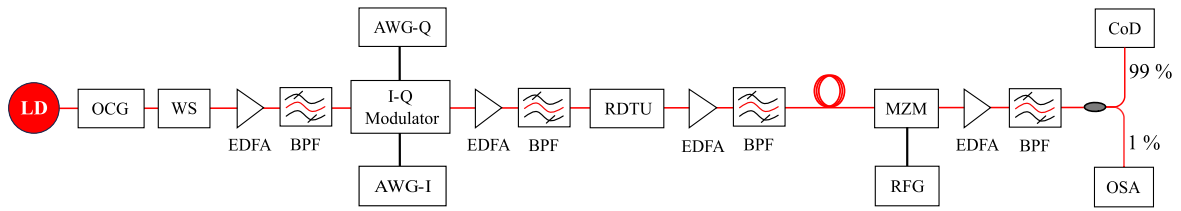
Fig. 2.   Experimental setup for high-bandwidth signal detection. LD: laser diode, OCG: optical comb generator, WS: waveshaper, EDFA: erbium-doped fiber amplifier, BPF: bandpass filter, RDTU: reconfigurable dispersion test unit, OSA: optical spectrum analyzer, RFG: radio frequency generator, AWG: arbitrary waveform generator.

with a spacing of 25 GHz were used for signal generation. On each of these 25 lines the same 24 GBd Nyquist QPSK signal is modulated by a Tektronix OM5110 Optical Transmitter. In order to analyse the data of the single slices without post processing, the 24 GBd slice consists of three multiplexed 8 GBd QPSK Nyquist channels, each modulated with an independent pseudorandom binary sequence (PRBS-7) signal. Please note that this gives a 24 GBd Nyquist signal [24]. To decorrelate the data content, a dispersion of 567 ps/nm is incorporated, which corresponds to a transmission in a standard single mode fiber with a length of 32 km. Optical amplifiers followed by filters for amplified spontaneous emission noise reduction were used to compensate for the losses.

At the receiver, we were realizing just one single sub-branch of the concept presented in Fig. 1(a). Therefore, for each single measurement we are just measuring the 8 GBd sub-signal of one single slice. To accomplish this, the MZM was driven by an 8 GHz sinusoidal frequency and the bias of the modulator was set such that the carrier and sidebands after modulation have the same amplitude for a flat comb. Since the PRBS-7 used for signal generation is periodic, the whole information can be received by shifting the phase of the RF signal driving the MZM successively to $0°$, $120°$ and $240°$. By tuning the LO in the CoD, the information of all spectral slices can be received with a bandwidth of 4 GHz, without any filtering of individual slices. However, the bandwidth of the CoD for the experiments was 33 GHz and could not be changed. To reduce the bandwidth to 4 GHz, we were using an electronic software filter after the detection of the signal. Please note that a real low-bandwidth CoD and ADC would provide a much better SINAD [20]. A coherent modulation analyzer (Tektronix-OM1106) conducted the necessary DSP of the recorded waveforms in a real-time oscilloscope (Tektronix DPO73304). This allowed for the visualization of symbol constellations, eye diagrams and the measurement of performance metrics such as the Q-factor. Forward error correction, pre-distortion, dispersion compensation, or any other kind of signal post-processing were not employed in the experiment.

In the second set of experiments, the bandwidth of the individual slices was increased beyond the comb spacing. This allows for a transmission at a rate faster than the Nyquist limit. This was achieved by reducing the frequency spacing of a comb with 33 lines to 20 GHz and modulating each line with 22.5 GBd QPSK data. For the detection, the sampling MZM was driven by a 7.5 GHz sinusoidal frequency. Here again, due to the bandwidth of our real-time oscilloscope of 33 GHz, a digital low-pass filter with a bandwidth of 3.75 GHz was used

to emulate a low-bandwidth device and the signal processing of the detection device for the measurement of the signals was incorporated. No additional signal post-processing was used. As we will show, the information can be detected from the high-bandwidth signals without any filters. But, since the output power of the laser diode is spread over the whole bandwidth, the optical signal-to-noise ratio (OSNR) of the generated high-bandwidth signals is quite low. Therefore, for the bit error rate (BER) measurement, we were using a 25 GHz optical filter and subsequent amplification before the coherent detection. Please note that this is 5 GHz broader than the single slice for the FTN signal. A Gaussian white noise was then added to the signal and the noise level was tuned with a variable optical attenuator.

B. Results

The comb for the 1.2 Tbit/s signal with 25 lines and 25 GHz spacing had a flatness of less than 1 dB as shown in Fig. 3(a). The spectrum of the transmitted signal, after modulation with 600 GBd QPSK data and an overall bandwidth of 624 GHz is depicted in Fig. 3(b). Each slice was modulated with 24 GBd data, since this defines the maximum of our equipment. Therefore, the slices have a rectangular spectrum, transmitting data with the theoretically maximum symbol rate of 24 GBd in a rectangular optical bandwidth of 24 GHz. However, since the comb spacing is 25 GHz and the resolution of the OSA in our experiments is 4 GHz, an intensity drop between the slices of around 2 dB can be seen.

For analysing the method, the sub-signals for the slices at the edges and in the center of the 624 GHz spectrum have been detected without filtering by tuning the frequency of the LO at the coherent receiver (193.1 THz, 193.7 THz and 193.4 THz), respectively. At an OSNR of 12 dB, the three sub-signals were received with a Q-factor of around 15 dB. The eye and constellation diagrams after the detection are shown in Fig. 3(c). The whole information of each slice can be retrieved by switching the phase of the RF signal driving the sampling modulator ($0°$, $120°$ and $240°$). In Fig. 4, the OSNR sensitivity of the sub-signals is characterized. As mentioned before, for this measurement the slices are optically filtered and amplified with an erbium-doped fiber amplifier followed by a sweep of the noise level by adding a Gaussian white noise to the filtered slices. The inset in Fig. 4 shows the eye and constellation diagrams from one of the sub-signals of the slice with the lowest center frequency (left of the spectrum) at an OSNR of 27.5 dB. The BER values in Fig. 4 are an estimate based on the measured Q-factor (in linear scale) of
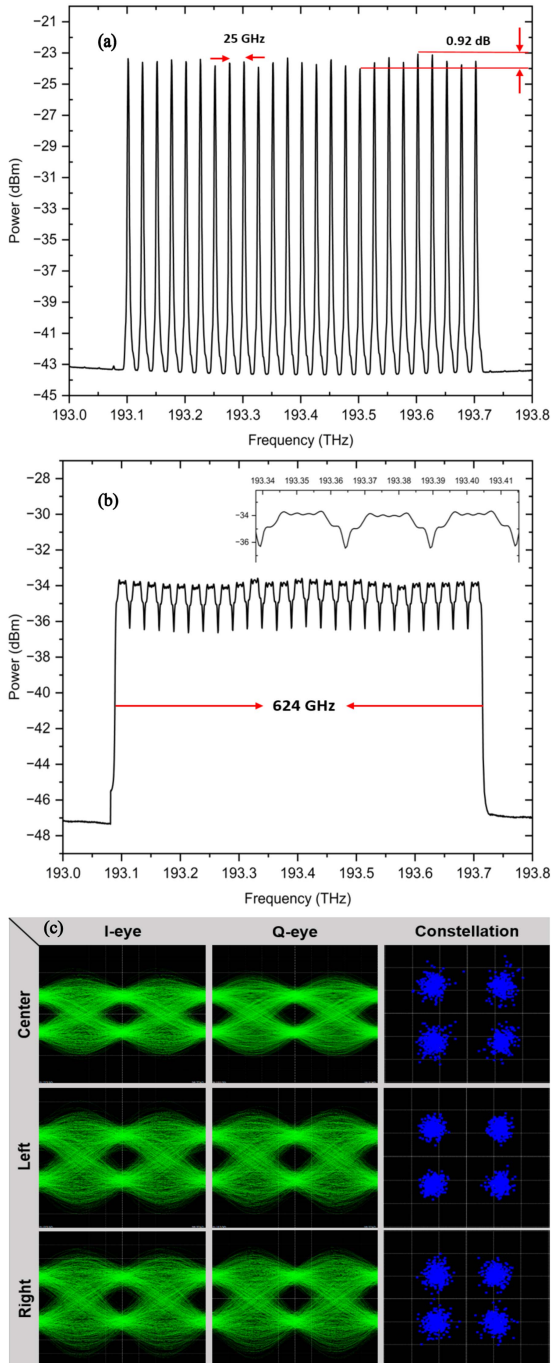
Fig. 3. Frequency comb (a) and signal spectrum (b) of bandwidth 624 GHz for Nyquist data transmission. The inset in (b) shows the spectral slices at the center of the transmitted spectrum. The OSA resolution was set to 4 GHz. The eye and constellation diagrams for one of the received sub-signals (8 GBd out of 24 GBd) of the slices at the center and edges of the transmitted spectrum are shown in (c).

the detected signal. Since for higher Q-factors a very long record length is necessary to measure the associated BER, the following relationship is used to plot the BER curves: $\text{BER}_{est} \approx \frac{1}{2}\text{erfc}\left(\frac{Q}{\sqrt{2}}\right)$ [25].

For demonstrating FTN transmission, an optical frequency comb of 33 lines with 20 GHz spacing was used, as shown in Fig. 5(a). Each comb line was modulated with 22.5 GBd
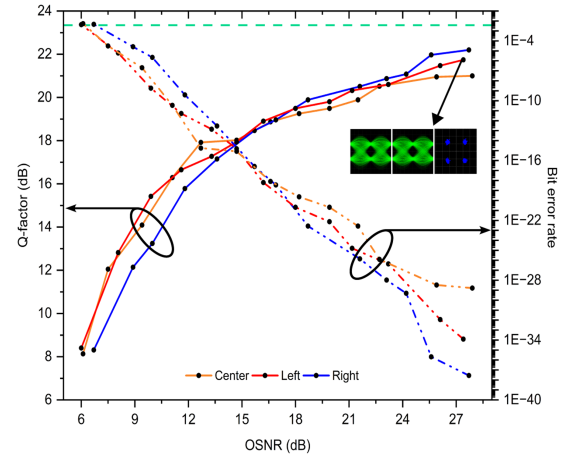

Fig. 4. Q-factor performance against OSNR (solid curves) for one of the sub-signals of the slices at the edges and center of the 624 GHz signal. The eye and constellation diagram for one of the sub-signals of the slice at 193.1 THz, received with a Q-factor of 22.2 dB, is shown in the inset, estimated BER (dotted), hard decision FEC limit (3.8E-3, green dashed).

(3×7.5 GBd Nyquist QPSK data), which corresponds to a rectangular bandwidth of 22.5 GHz. Therefore, the spectral overlap between adjacent slices is 22%. The overall signal spectrum has a bandwidth of 662.5 GHz and the QPSK symbol rate is 742.5 GBd, resulting in a data rate of 1.485 Tbit/s. As can be seen from Fig. 5(b), there are peaks in between the different spectral slices. These peaks are a kind of interference at the spectral overlap of two adjacent slices. The eye and constellation diagrams after detection of the sub-signals for the slices at the edges and the center without an optical filter are shown in Fig. 5(c), respectively, the Q-factor was around 13.2 dB. The measurement of the Q-factor and calculated BER against OSNR (again with a 25 GHz optical filter and subsequent amplification) is depicted in Fig. 6. The inset shows the eye and constellation diagram for one of the sub-signals of the slice located at the left edge of the transmitted spectrum, with an OSNR of 24.2 dB.

IV. DISCUSSION

The presented receiver has successfully achieved a data reception rate exceeding 1 Tbit/s with a detector bandwidth of just 4 GHz. No high-quality filters, pulse sources, specialized optical or electronic equipment or non-linear optical effects were needed. Additionally, the delay between the parallel branches for orthogonality can be finely adjusted through the phase of the RF driving the modulator and no additional optical delay lines and corresponding compensations for mismatches in the delay or amplitude are required. Therefore, the integration of the system seems to be straightforward.

To address the escalating need for greater channel capacity in communication networks, we also explored FTN signaling. In FTN signaling the data is transmitted at a symbol rate faster than the Nyquist limit. This enhances the spectral efficiency and achieves higher channel capacity compared to the Nyquist signal. Several approaches towards FTN signaling have been reported in [26], [27], [28]. Here, we have experimentally demonstrated the reception of FTN signals with a spectral
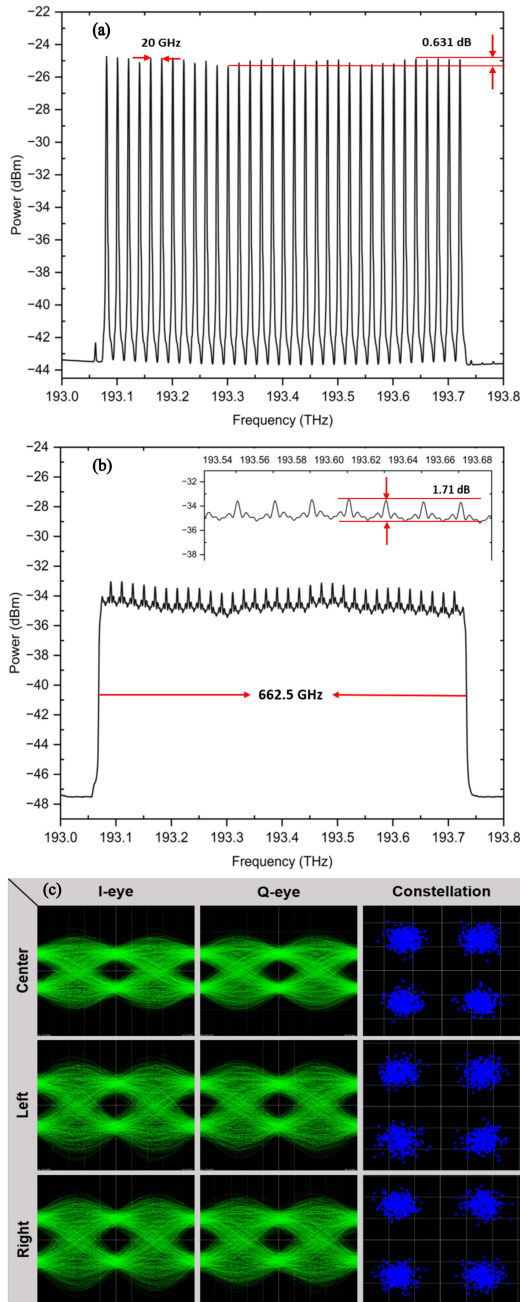
Fig. 5. Frequency comb (a) and signal spectrum (b) with a bandwidth of 662.5 GHz for FTN data transmission. The inset in (b) shows a part of the spectrum at the center (OSA resolution, 4 GHz). The eye and constellation diagrams for one of the sub-signals (7.5 GBd out of 22.5 GBd) of the slices at the center and edges of the transmitted spectrum are shown in (c).

overlap of 22%. This reduces the Q-factor, however, a pre- or post-processing of the signals was not necessary.

Since the detection bandwidth is reduced to 4 GHz, the SINAD and ENOB of the detection is improved in comparison to the direct detection of the high-bandwidth signal. The enhancement mainly results from the reduced influence of the aperture jitter [29]. A detailed analysis and experimental verification is reported in [20]. However, since there are no ADC with a bandwidth of 600 GHz, a direct analysis of the SINAD and ENOB improvement is not possible for the presented work.
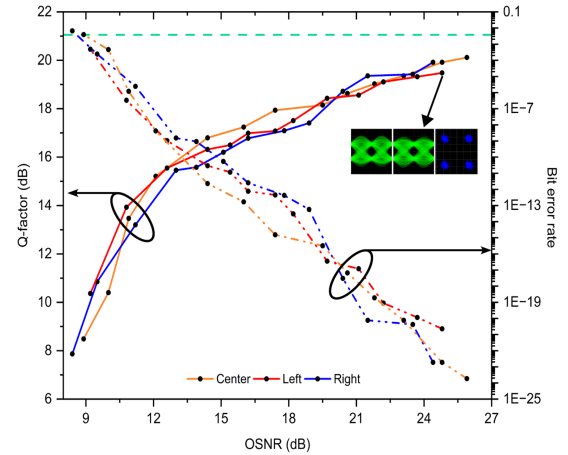

Fig. 6. Q-factor performance against OSNR (solid curves) for one of the sub-signals of the slices at the edges and center of the 662.5 GHz signal with FTN transmission. The eye and constellation diagram, for one of the sub-signals, of the slice at 193.1 THz received with a Q-factor of 19.4 dB is shown in the inset. The estimated BER is shown with dotted curves and the hard decision FEC limit (3.8E-3) is marked with a green dashed line.

Instead, we could define the improvement for the single slice. But, if spectrum slicing is used, the slice has to be filtered out of the high-bandwidth signal by an optical filter, which may lead to additional distortions. Given that an ideal rectangular filter is available and the filtered slice is measured with an ADC with a bandwidth of 12 GHz, its ENOB and SINAD would be lower than by the detection with our method. In [30] it was demonstrated, for instance, that detecting a 24 GBd (24 GHz) signal with 4 GHz ADC in three branches shows a Q-factor improvement of 2.2 dB. This improved quality of the detected signal may result in a lower requirement for power consumption in any following signal processing.

V. CONCLUSION

In conclusion, we have experimentally demonstrated the reception of a terabit FTN superchannel with up to 1.485 Tbit/s data rate with 4 GHz electronics. The bandwidth requirement for signal detection was reduced by sampling the signals in parallel branches with orthogonal sinc-pulse sequences. The simultaneous sampling and frequency comb generation by an MZM, with all parameters adjusted and controlled via the RF driving the modulator is highly flexible in terms of the change of bandwidth and sampling rate. Moreover, just standard and low-bandwidth optical and electronic components were employed. Therefore, this method maybe a viable solution for next-generation Tbps data centers as well as for optical and wireless networks.

REFERENCES

[1] J. Yu and J. Zhang, "Recent progress on high-speed optical transmission," *Digit. Commun. Netw.*, vol. 2, no. 2, pp. 65–76, 2016.

[2] A. Feldmann et al., "Implications of the COVID-19 pandemic on the internet traffic," in *Proc. Broadband Coverage Germany; 15th ITG- Symp.*, 2021, pp. 1–5.

[3] M. Nagatani et al., "110-GHz-Bandwidth InP-HBT AMUX/ADEMUX circuits for Beyond-1-Tb/s/ch digital coherent optical transceivers," in *Proc. IEEE Custom Integr. Circuits Conf.*, 2022, pp. 1–8.

[4] I. F. Akyildiz, A. Kak, and S. Nie, "6G and beyond: The future of wireless communications systems," *IEEE Access*, vol. 8, pp. 133995–134030, 2020.

[5] I. F. Akyildiz, C. Han, Z. Hu, S. Nie, and J. M. Jornet, "Terahertz band communication: An old problem revisited and research directions for the next decade," *IEEE Trans. Commun.*, vol. 70, no. 6, pp. 4250–4285, Jun. 2022.

[6] P. Shao et al., "Preparation and transmission characteristics of seven-core few-mode fiber with low loss and low inter-core crosstalk," *Opt. Exp.*, vol. 30, no. 15, pp. 27746–27762, Jul. 2022.

[7] J. Baliga, R. Ayre, K. Hinton, W. V. Sorin, and R. S. Tucker, "Energy consumption in optical IP networks," *J. Lightw. Technol.*, vol. 27, no. 13, pp. 2391–2403, Jul. 2009.

[8] A. Matsushita, M. Nakamura, S. Yamamoto, F. Hamaoka, and Y. Kisaka, "41-Tbps C-band WDM transmission with 10-bps/Hz spectral efficiency using 1-Tbps/λ signals," *J. Lightw. Technol.*, vol. 38, no. 11, pp. 2905–2911, 2020.

[9] F. Buchali, V. Lauinger, M. Chagnon, K. Schuh, and V. Aref, "CMOS DAC supported 1.1Tb/s/λ DWDM transmission at 9.8 bit/s/Hz over DCI distances," *J. Lightw. Technol.*, vol. 39, no. 4, pp. 1171–1178, 2021.

[10] D. Che and X. Chen, "Achievable rate comparison between probabilistically-shaped single-carrier and entropy-loaded multi-carrier signaling in a bandwidth-limited 1-Tb/s coherent system," in *Proc. IEEE Opt. Fiber Commun. Conf. Exhib.*, 2021, pp. 1–3.

[11] H. Yamazaki et al., "Transmission of 160.7-GBaud 1.64-Tbps signal using phase-interleaving optical modulator and digital spectral weaver," *J. Lightw. Technol.*, vol. 41, no. 11, pp. 3382–3388, 2023.

[12] T. Schneider, "Toward terabit receivers for optical and wireless communications," *IEEE Commun. Mag.*, vol. 61, no. 8, pp. 169–174, Aug. 2023.

[13] X. Xie et al., "Photonic microwave signals with zeptosecond-level absolute timing noise," *Nature Photon.*, vol. 11, no. 1, pp. 44–47, Jan. 2017.

[14] R. Walden, "Analog-to-digital converter survey and analysis," *IEEE J. Sel. Areas Commun.*, vol. 17, no. 4, pp. 539–550, Apr. 1999.

[15] N. K. Fontaine, R. P. Scott, L. Zhou, F. M. Soares, J. Heritage, and S. Yoo, "Real-time full-field arbitrary optical waveform measurement," *Nature Photon.*, vol. 4, no. 4, pp. 248–254, 2010.

[16] N. K. Fontaine et al., "228-GHz coherent receiver using digital optical bandwidth interleaving and reception of 214-GBd (856-Gb/s) PDM-QPSK," in *Proc. Eur. Conf. Exhib. Opt. Commun.*, 2012, pp. Th-3.

[17] D. Drayss et al., "Slice-less optical arbitrary waveform measurement (OAWM) in a bandwidth of more than 600GHz," in *Proc. Opt. Fiber Commun. Conf. Exhib.*, 2022, pp. 1–3.

[18] A. Misra, J. Meier, S. Preussler, K. Singh, and T. Schneider, "Agnostic sampling transceiver," *Opt. Exp.*, vol. 29, no. 10, pp. 14828–14840, May 2021.

[19] J. Meier, K. Singh, A. Misra, S. Preußler, J. C. Scheytt, and T. Schneider, "High-bandwidth arbitrary signal detection using low-speed electronics," *IEEE Photon. J.*, vol. 14, no. 2, Apr. 2022, Art. no. 5515207.

[20] Y. Mandalawi, J. Meier, K. Singh, M. I. Hosni, S. De, and T. Schneider, "Analysis of bandwidth reduction and resolution improvement for photonics-assisted ADC," *J. Lightw. Technol.*, vol. 41, no. 19, pp. 6225–6234, 2023.

[21] M. A. Soto et al., "Optical sinc-shaped Nyquist pulses of exceptional quality," *Nature Commun.*, vol. 4, no. 1, Dec. 2013, Art. no. 2898.

[22] M. A. Soto et al., "Generation of Nyquist sinc pulses using intensity modulators," in *Proc. CLEO*, 2013, pp. 1–2.

[23] C. E. Shannon, "A mathematical theory of communication," *Bell Syst. Tech. J.*, vol. 27, no. 3, pp. 379–423, 1948.

[24] A. Misra et al., "Reconfigurable and real-time high-bandwidth Nyquist signal detection with low-bandwidth in silicon photonics," *Opt. Exp.*, vol. 30, no. 8, pp. 13776–13789, Apr. 2022.

[25] R. Schmogrow et al., "Error vector magnitude as a performance measure for advanced modulation formats," *IEEE Photon. Technol. Lett.*, vol. 24, no. 1, pp. 61–63, Jan. 2012.

[26] J. Zhou et al., "Capacity limit for faster-than-Nyquist non-orthogonal frequency-division multiplexing signaling," *Sci. Rep.*, vol. 7, no. 1, 2017, Art. no. 3380.

[27] L. Li, Y. Lu, L. Liu, D. Chang, Z. Xiao, and Y. Wei, "20–224Gbps (56Gbaud) PDM-QPSK transmission in 50GHz grid over 3040km G.652 fiber and EDFA only link using Soft Output Faster than Nyquist Technology," in *Proc. OFC*, 2014, pp. 1–3.

[28] L. Liu, L. Li, and Y. Lu, "Detection of 56GBaud PDM-QPSK generated by commercial CMOS DAC with 11GHz analog bandwidth," in *Proc. IEEE Eur. Conf. Opt. Commun.*, 2014, pp. 1–3.

[29] A. Khilo et al., "Photonic ADC: Overcoming the bottleneck of electronic jitter," *Opt. Exp.*, vol. 20, no. 4, pp. 4454–4469, 2012.

[30] M. I. Hosni, Y. Mandalawi, J. Meier, K. Singh, A. M. Mokhtar, and T. Schneider, "Low-bandwidth photonics-assisted receiver for broadbandwidth wireless signals," *IEEE Access*, vol. 11, pp. 44260–44266, 2023.